Clim Dyn
DOI 10.1007/s00382-013-1794-9

Soil moisture-temperature feedbacks at meso-scale during summer heat waves over Western Europe

Marc Stéfanon · Philippe Drobinski · Fabio D'Andrea · Cindy Lebeaupin-Brossier · Sophie Bastin

Received: 22 October 2012 / Accepted: 25 April 2013

Abstract This paper investigates the impact of soil moisture-temperature feedback during heatwaves occurring over France between 1989 and 2008. Two simulations of the weather research and forecasting regional model have been analysed, with two different land-surface models. One resolves the hydrology and is able to simulate summer dryness, while the other prescribes constant and high soil moisture and hence no soil moisture deficit. The sensitivity analysis conducted for all heatwave episodes highlights different soil moisture-temperature responses (1) over low-elevation plains, (2) over mountains and (3) over coastal regions. In the plains, soil moisture deficit induces less evapotranspiration and higher sensible heat flux. This has the effect of heating the planetary boundary layer and at the same time of creating a general condition of higher convective instability and a slight increase of shallow cloud cover. A positive feedback is created which increases the temperature anomaly during the heatwaves. In mountainous regions, enhanced heat fluxes over dry soil reinforce upslope winds producing strong vertical motion over the mountain slope, first triggered by thermal convection. This, jointly to the instability conditions, favors convection triggering and produces clouds and precipitation over the mountains, reducing the temperature anomaly. In coastal regions, dry soil enhances land/sea thermal contrast, strengthening sea-breeze circulation and moist cold marine air advection. This damps the magnitude of the heatwave temperature anomaly in coastal areas, expecially near the Mediterranean coast. Hence, along with heating in the plains, soil dryness can also have a significant cooling effect over mountains and coastal regions due to meso-scale circulations.

Keywords Heatwaves · Droughts · Mediterranean climate · HyMeX · MED-CORDEX · Hydrological cycle · Meso-scale circulations

M. Stéfanon (✉) · P. Drobinski · F. D'Andrea
Institut Pierre Simon Laplace, Laboratoire de Météorologie Dynamique, CNRS/Ecole Polytechnique/ENS/UPMC, Palaiseau, France
e-mail: marc.stefanon@lmd.polytechnique.fr

C. Lebeaupin-Brossier
CNRM-GAME, Météo-France and CNRS, Toulouse, France

S. Bastin
Institut Pierre Simon Laplace, Laboratoire Atmosphères, Milieux, Observations Spatiales, CNRS/UVSQ/UPMC, Guyancourt, France

1 Introduction

In the Euro-Mediterranean region Heatwaves may become more frequent, longer and more intense in the future (Easterling et al. 2000; Beniston 2004; Della-Marta et al. 2007), raising worries on the the impact of such extreme events on the economic activities and on public health (Fouillet et al. 2006).

Heatwaves in Western and Central Europe are generally preceded by a rainfall deficit in Southern Europe (Vautard et al. 2007; Stéfanon et al. 2012a; Zampieri et al. 2009), showing evidence of a possible soil-moisture temperature feedback. Indeed, given that soil moisture observations are scarce and scattered in time and space, climate models and rainfall analyses are generally used as a proxy (Vautard et al. 2007), to evaluate these interactions. A rainfall deficit creates a lack of soil moisture which induces less evapotranspiration. This can lead to a drier atmosphere with less clouds and precipitations. This effect can be local or remote, with the advection of dry and cloudless air from Mediterranean to Northern Europe during the spring.

Published online: 08 May 2013

In fact, Heatwaves and droughts are intrinsically linked through the strong coupling within the Earth's energy and water cycle (Beljaars et al. 1996; D'Andrea et al. 2006; Fischer et al. 2007; Vautard et al. 2007), and the several mechanisms that compose them. The specific case of the summer 2003 Heatwave has been investigated numerically by Fischer et al. (2007a, b). They found that, uncoupling the atmospheric component of a model by imposing a climatological soil moisture reduced the summer temperature anomaly by 40 % over certain regions, and that the land atmosphere coupling accounted for 50–80 % of the total number of hot days during the last major European Heatwaves (1976–1994–2003–2005).

The study of the coupling of soil moisture with temperature and precipitation is far from being a recent research activity (see Seneviratne et al. 2010 for an extensive review), but substantial uncertainities on the basic physical mechanism at play at different time and space scales remain. While it is somewhat straightforward that local-scale evaporative recycling of soil moisture enhances precipitation, soil moisture can also alter the planetary boundary layer (PBL) dynamics and thermodynamics, modifying a number of feedbacks involving turbulent and radiative fluxes and clouds. This may result in a positive feedback of soil moisture on precipitation, or sometimes on a negative one (Betts et al. 1996; Schär et al. 1999; Pal and Eltahir 2001; Findell and Eltahir 2003; Couvreux et al. 2009; Guichard et al. 2009; Hohenegger et al. 2009; Siqueira et al. 2009; Santanello Jr et al. 2011; Couvreux et al. 2012).

At the mesoscale, land-surface details, including soil moisture patchiness (Taylor et al. 2007), vegetation heterogeneity (e.g. Chagnon et al. 2004; Wang et al. 2009; Stéfanon et al. 2012b) and orography, are believed to strongly modify the influence of soil moisture on temperature, cloudiness and precipitation. For example, in mid-latitudes and dry atmospheric conditions, Rabin et al. (1990) observed with satellite imagery an upward trend in cloudiness over regions characterized by higher sensible heat flux than adjacent areas. It has also been shown that in the Sahel, soil moisture gradients can induce meso-scale circulations creating moisture convergence and hence increased convection over dry areas (Taylor et al. 2007). Hohenegger et al. (2009) conducted a sensitivity experiments for July 2006 over the Alpine region with a a cloud resolving model run at 2.2 km resolution. They show that a drier soil yields an enhancement of sensible heat flux, and thermals able to pierce the layer of stable air above the boundary layer, ultimately causing a negative soil moisture-precipitation feedback.

This article investigates this complex behavior of the surface-atmosphere coupling with a regional meso-scale model for the specific cases of the Heatwaves occurring between 1989 and 2008 over Western Europe (Fig. 1). One fundamental motivation is to investigate the role of meso-scale boundary layer dynamics generally produced by the land-surface heterogeneity (e.g. mountainous or coastal regions) on the sign of the soil moisture-precipitation feedback and thus on the magnitude of the temperature anomaly of the Heatwave. Western Europe is dominated by several complex terrain features, including several mountain ranges (Pyrénées, Massif Central, and the Alps), jagged coastlines, and land cover heterogeneity. This causes meso-scale circulation in the boundary layer, such as valley winds (Drobinski et al. 2001, 2005; Guénard et al. 2005, 2006) or inland and sea breezes (Bastin and Drobinski 2005, 2006; Drobinski et al. 2006) which play a key role in the water vapor transport (Bastin et al. 2005a, b, 2007). It is also sensitive to soil moisture-temperature coupling (Seneviratne et al. 2006).

The approach consists of a sensitivity analysis between two 20-year simulations performed at 20 km resolution with the Weather Research and Forecasting (WRF) model over the Mediterranean basin in the framework of the CORDEX (COordinated Downscaling Experiment; Giorgi et al. (2009)—MED-CORDEX being the Mediterranean focus of CORDEX) and HyMeX (Hydrological cycle in the Mediterranean experiment; see international science plan

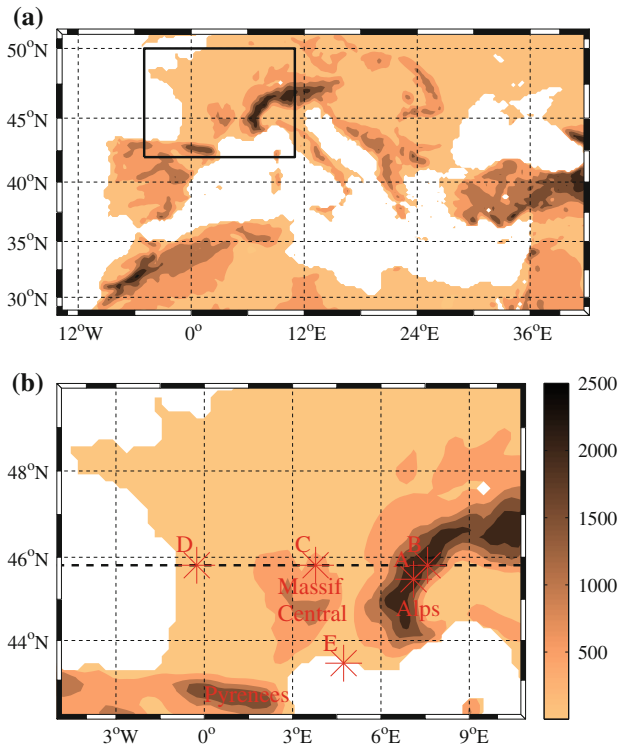

Fig. 1 **a** Domain of the HyMeX/MED-CORDEX simulations covering Europe and the Mediterranean region. The *rectangle* indicates the domain of investigation of this study with details in (**b**). In **b**, the *dashed line* and the *letters* indicate the location of cross sections and point analysis performed in Sect. 5. The *color shading* indicates the topography elevation

on http://www.hymex.org; see also Drobinski et al. 2009, 2010) programs. The two simulations perform a dynamical downscaling of the ERA-interim data (Simons et al. 2007). In one simulation, soil moisture can evolve freely by using a sophisticated land-surface model, while in the other, the soil moisture availability is prescribed and set to climatological wintertime value preventing any soil moisture deficit situation. They are used to identify the dynamical meso-scale processes controlling the feedback loops and their local contribution to the temperature anomaly associated with the heat-wave events occurring over the 1989–2008 period.

This paper is organized as follows. After the introduction in Sect. 1, the numerical model, its configuration and set-up, as well as the validation dataset are detailed in Sect. 2. The comparison with validation dataset and a detailed analysis of the hydrological cycle as simulated in the two HyMeX/MED-CORDEX simulations are provided in Sects. 3 and 4. Section 5 describes the physical processes involved in the boundary layer structure and the surface energy budget. The discussion and conclusion are given in Sect. 6.

2 Model and data

2.1 Numerical model

We use the Weather Research and Forecasting (WRF) model of the National Center for Atmospheric Research (NCAR) (Skamarock et al. 2008). The regional domain has a 20 km horizontal resolution (249 × 129 grid points) and covers the Euro-Mediterranean region (Fig. 1). The model has 28 sigma-levels in the vertical. Initial and lateral conditions are from the ERA-Interim reanalysis of the European Centre for Mean-range Weather Forecasts (ECMWF) (Dee et al. 2011; Simons et al. 2007) provided every 6 h with a 0.75° resolution. A complete set of physics parameterizations is used with WRF, the Single-Moment 5-class microphysical scheme (Hong et al. 2004), the new Kain-Fritsch convection scheme (Kain 2004), the Yonsei University (YSU) planetary boundary layer (PBL) scheme (Noh et al. 2003) and a parameterization based on the similarity theory (Monin and Obukhov 1954) for the turbulent fluxes. The radiative scheme is based on the Rapid Radiative Transfer Model (RRTM) (Mlawer et al. 1997) and the Dudhia (1989) parameterization for the longwaves and shortwaves radiation, respectively. The lower boundary conditions of the WRF model are provided by the land surface model (LSM). In this study, we use the thermal diffusion scheme (SLab scheme) and the rapid update cycle model LSM (RUC) (see hereafter for details).

The Mediterranean domain is sufficiently small to produce strong control of the simulations by the boundary conditions (Omrani et al. 2012) and avoid unrealistic departures from the driving fields. In addition indiscriminate nudging is applied with a nudging coefficient of $5 \times 10^{-5}\mathrm{s}^{-1}$ for temperature, humidity and velocity components above the planetary boundary layer (Stauffer and Seaman 1990; Salameh et al. 2010).

2.1.1 *The land surface models*

The role of the LSM is to compute heat and moisture flux over land but also roughness length or leaf area index and other canopy properties. Therefore it determines the partitioning between latent and sensible heat flux, of high importance for extreme events.

WRF can use several LSMs with various degrees of sophistication. Hereafter we will detail only the LSMs used in the present article, the rapid update cycle model LSM (RUC) (Smirnova et al. 1997, 2000b) and the thermal diffusion scheme (SLab scheme) (Skamarock et al. 2008; Eckel 2002). The two differents LSMs were chosen, one sophisticated-a full model of soil hydrology-and another rather basic, was a perfect testbed for sensitivity to soil conditions.

The SLab scheme is a simple model based on the MM5 soil temperature model. Soil moisture is prescribed at each grid point by a soil moisture availability coefficient M which depends on the land use and takes different values for winter and summer (soil moisture availability is much larger during winter than during summer). Soil moisture availability, used to compute latent heat flux, has been calibrated from climatologies of soil moisture and so do not represent a specific situation like the summer 2003 drought. For our sensitivity experiment, soil moisture availability has been prescribed to its wintertime values, thus preventing the simulation of soil moisture deficit situations. In the SLab model, evapotranspiration E is calculated from a bulk formulation of the Monin-Obukhov similarity theory and is given by:

$$E = MC_H V_1 \rho \times (q_0^* - q_1)$$

where C_H,V_1 and ρ are the drag coefficient for heat fluxes, wind speed at first grid level and the air density, respectively. The quantities q_1 and q_0^* are the mixing ratio at first grid level and the saturation mixing ratio at the surface, respectively.

The RUC LSM is used in the operational version of the mesoscale analysis and prediction system (MAPS, Bleck and Benjamin 1993) operated at the National Oceanic and Atmospheric Administration (NOAA). It solves the vertical diffusive equation of soil moisture over six layers with bottom level at 3 m. It includes the treatment of soil

moisture diffusion, runoff, evapotranspiration and precipitation. Underground water transport processes are implemented as described in Philip and de Vries (1957):

$$\frac{\partial \eta}{\partial t} = \frac{\partial}{\partial z}\left(D_\eta \frac{\partial \eta}{\partial z}\right) + \frac{\partial K_\eta}{\partial z}$$

where η, D_η, K_η are the volumetric water content of soil, soil moisture diffusion and hydraulic conductivity, respectively. The evapotranspiration has three components. Direct evaporation from bare ground, evaporation of interception loss from canopy and vegetation transpiration including water from root zone. Transpiration is formulated by Mahrt and Pan (1984) and is proportional to the potential evaporation and transpiration rate function, the ratio between available soil moisture content to the available moisture content at field capacity. Root distribution is supposed uniform and constant in the vertical and there is no horizontal water motion.

2.1.2 The convective parameterization scheme

The Kain–Fritsch convective parameterization scheme from Kain (1993, 2004) (hereafter referred as KF) determines the physical processes by which the convective inhibition energy (CIN) is removed and the convective available energy (CAPE) activated when convection develops. It is also a mass flux scheme, based on CAPE, which calculates transfers of mass in updrafts and downdrafts. It uses an entrainment and detrainment rate calculated from the updraft mixing properties with the surrounding environment. Its closure equation is function of the CAPE, and is activated when at least 90 % of the CAPE is removed. CAPE is calculated from an entraining parcel. The trigger control depends strongly on background vertical motion and includes additional boundary layer criteria.

Deep convection is produced when the air parcel can be lifted over a minimum depth (typically 3–4 km) which varies as a function the cloud base temperature. Compared to a preset constant depth, this approach gives more realistic results (Kain 2004). Shallow convection is allowed and activated when all criteria for deep convection are present except for the imposed minimum depth. In this case, the mass flux is based on turbulent kinetic energy instead of CAPE. Convective precipitation is given by the residual condensate between updraft detrainment and downdraft evaporation.

A number of convection parameterizations are not able to capture the main features of deep convection (time and intensity) and do not correctly represent soil moisture-precipitation feedbacks (Bechtold et al. 2001; Guichard et al. 2004). However KF scheme proved to correctly simulate the soil moisture-precipitation feedbacks, with results similar to cloud resolving models in idealized cases (Hohenegger et al. 2009).

2.1.3 The planetary boundary layer scheme

The Yosei University scheme (YSU) scheme is a modified version of the medium-range forecast (MRF) scheme (Hong and Pan 1996; Troen and Mahrt 1986). Its major modification is the explicit treatment of entrainment at the top of the boundary layer which is proportional to surface buoyancy. Overall, the depth of the PBL is determined by the thermal profile where its top is set to the maximum entrainment layer. Vertical diffusion is dependent of the Richardson number in the free atmosphere. In Hong et al. (2006), there is a detailed description of the scheme as also a MRF-YSU comparison based on WRF simulations.

2.1.4 Numerical simulations

Two simulations have been performed with WRF driven by ERA-Interim at 20 km resolution, with the RUC and SLab LSMs (hereafter referred as RUC and SLab simulations, respectively). The two simulations have been run from January 1989 to December 2008 on a Mediterranean domain with a SST prescribed from ERA-Interim. These simulations have been performed in the context of the HyMeX and MED-CORDEX framework. The CORDEX program was instituted by the World Climate Research Program (WCRP) to develop downscaled regional climate change projections at user-relevant scales for all terrestrial regions of the world. HyMeX is a program dedicated to the hydrological cycle and related processes in the Mediterranean (http://www.hymex.org).

The simulation performed with RUC LSM simulates the temporal and spatial variations of soil moisture, including drought conditions. Conversely, the simulation performed with SLab LSM are forced to keep high soil moisture values which are land-use dependent, close to field capacity and constant with time. The landuse is aggregated from the United States Geographical Survey data with 10-minute grid spacing, and is constant through time. The soil texture comes from the State Soil Geographic Database (STATSGO) with a $1° \times 2°$ grid resolution, developed by the U.S. Department of Agriculture-Natural Resources Conservation Service (Bradley 2003). These simulations are compared to provide an estimate of the soil moisture contribution to the meso-scale spatial variability and magnitude of the temperature anomaly associated with Heatwaves.

The analysis is performed over a domain centered over France (Fig. 1). This domain is located within one of the areas where Heatwaves appear recurrently and where soil–atmosphere interactions are key elements of Heatwave

preconditioning (Vautard et al. 2007; Fischer et al. 2007a, b; Stéfanon et al. 2012a). It is a region of strong complexity with various land uses inducing pronounced inland surface heterogeneities, with elevated mountain ranges (Pyrénées, Massif Central, French Alps), large flat plains and extensive coastal regions. It is also located on either side of the 46°N parallel which corresponds to a sharp transitional zone between the Mediterranean dry and the European continental climates (Köppen 1936; Peel et al. 2007).

2.2 Observational data

For our model evaluation, a gridded version (E-OBS 3.0) of the European Climate Assessment & Data (ECA&D) is used for continental air temperature (mean, minimum and maximum) and precipitation (Tank et al. 2002; Haylock et al. 2008). The grid resolution is 0.5° × 0.5° and the data span from 1950 to 2009. Data observations were aggregated from several weather stations and gridded using an interpolation procedure combining spline interpolation and kriging. The interpolation smoothes the peak values inducing a 1.1 °C decrease of the median value of maximum temperature, if we consider an extreme event with a ten year return period (Haylock et al. 2008).

3 Representation of Heatwaves in the RUC and SLab simulations

Figure 2 shows the cumulative distribution function of summer daily maximum temperature and the corresponding anomaly with respect to the 20-year climatology from ECA&D data and RUC and SLab simulations. Data are averaged over the domain (see rectangle in Fig. 1). It shows evidence of a weak warm bias around +0.5 °C between ECA&D and the RUC simulation and a large cold bias of about −4 °C in the SLab simulation. The standard deviation of the temperature anomaly is slightly higher than ECA&D in the RUC simulation (3.64 and 3.77 °C, respectively) and lower in the SLab simulation (2.81 °C).

This suggests that soil moisture strongly controls the near-surface temperature mean and the amplitude of the temperature variability. The synoptic variability, which is similar in the two simulations, also drives the time evolution of the near surface temperature. Indeed, the temporal correlation coefficient of the summer daily maximum temperature averaged over the domain of investigation is 0.99 between the RUC simulation and ECA&D data and 0.97 between the SLab simulation and ECA&D data. Spatially, the patterns of the median of the summer daily maximum temperature display meso-scale variability (Fig. 3). Along the Mediterranean coast, in South Western France and in the Rhône and Aude valleys (between Alps and Massif Central and between Massif Central and Pyrenees, respectively), the RUC simulation is warmer by about +2 °C with respect to ECA&D data. The bias is close to 0 in lowlands, whereas the RUC simulation is colder by about −1 °C (and up to −3 °C) in mountainous regions. Regarding the SLab simulation, besides its strong negative bias with respect to ECA&D data (and the RUC simulation), the pattern is similar except over the mountains where the bias is much lower.

We now focus on the specific case of Heatwave events. The days when Heatwaves occur are defined as days during which the daily maximum temperature anomaly with respect to the climatology exceeds the 95th quantile. The 95th quantile of the summer temperature anomaly, which allows to remove the seasonal cycle, is calculated from the summer distribution (taken into account every day of June to August over the 1989–2008 period). The 95th quantile of the summer temperature anomaly are 5.55, 4.16 and 5.39 °C for RUC, SLab simulations, and ECA&D data, respectively. We thus obtain the dates of Heatwaves occurring between 1989 and 2008 (Fig. 4). RUC and Slab simulations and ECA&D data share 75 % of Heatwaves days. The number of overlapping Heatwaves days with ECA&D is 71 for the RUC simulation and 70 for the SLab simulations out a maximum of 92 days. However, when Heatwave days do not match between the RUC/SLab simulations and the ECA&D data, they still correspond to very hot days (>90th quantile). Over the 1989–2008 period, 2003 and 2006 are the warmest summers in terms of number of Heatwave days (Fig. 4) and temperature anomaly magnitude (not shown). The specific case of the summer 2003 Heatwave is now taken as an example of typical Western European Heatwave. The summer 2003 Heatwave simulated with the RUC and SLab LSMs is associated with a nearly identical 500-hPa geopotential height anomaly (less than 0.4 % difference) corresponding to a strong anticyclonic anomaly over Northern Europe, similar to the summer blocking situation of Cassou et al. (2005); Stéfanon et al. (2012a) (not shown). The spatial pattern of the 500-hPa geopotential height anomaly is strongly correlated to surface temperature anomaly Stéfanon et al. (2012a). Figure 5 (panels a, b and c) shows the 2003 temperature anomaly with respect to the climatology. It is centered mostly over North Western France and has a magnitude of about 5–6 °C in the Slab simulation with a peak over the Massif Central reaching 8 °C. The origin of 5–6 °C temperature anomaly can thus be considered mainly driven by the atmospheric blocking which inhibits cloud formation and increases incoming solar radiation at the surface. In the RUC simulation and ECA&D data, the surface temperature anomaly reaches about 8–9 °C. This anomaly includes both the impact of the anticyclonic

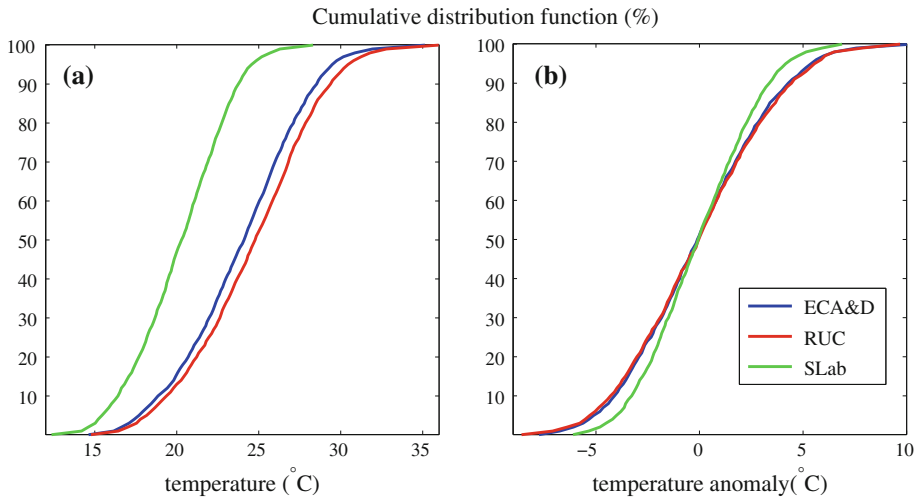

Fig. 2 Cumulative distribution function **a**–**b** of summer daily maximum temperature (**a**) and the summer daily maximum temperature anomaly (**b**) with respect to the 20-year climatology from ECA&D data and RUC and SLab simulations (summer corresponds to June–July–August, i.e. JJA). Data are averaged over the domain indicated in Fig. 1b

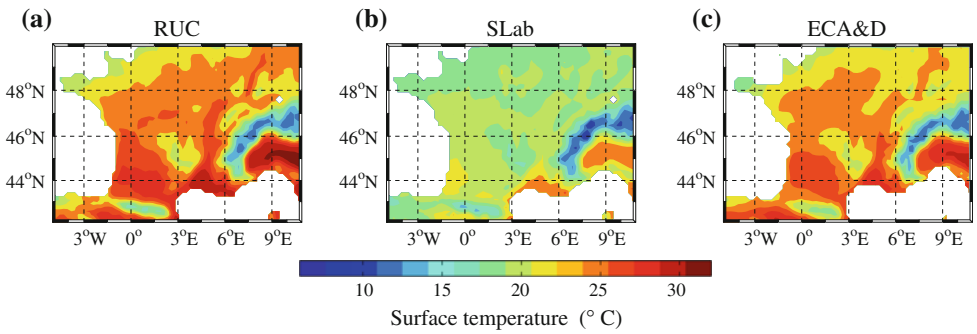

Fig. 3 Median of the summer daily maximum temperature over the 1989–2008 period for **a** the RUC simulation, **b** SLab and **c** ECA&D data

conditions and the soil moisture/temperature feedback effect. At first order, one can thus estimate the contribution to the temperature anomaly of the soil moisture/temperature feedback to about 3 °C.

Western European Heatwaves are also often correlated with a persistent precipitation deficit (Vautard et al. 2007; Stéfanon et al. 2012a). The year 2003 was a very dry year, even though interrupted intermittently by local and intense heavy rainfall producing floods (Fink et al. 2004; Christensen and Christensen 2003). The precipitation deficit of 2003 as reproduced by the RUC and SLab simulations and from the ECA&D data is shown in Fig. 5 (panels d, e and f). The overall deficit is accurately simulated. The patterns of RUC and SLab simulations are fairly similar. The RUC simulation displays a more severe rainfall deficit-averaged over the domain-of about -0.07 mm day^{-1} with respect to the SLab simulation. Note that the patterns of the temperature and rainfall anomalies of the summer 2003 Heatwave displayed in Fig. 5 are very similar to most other Heatwave situations occurring in France.

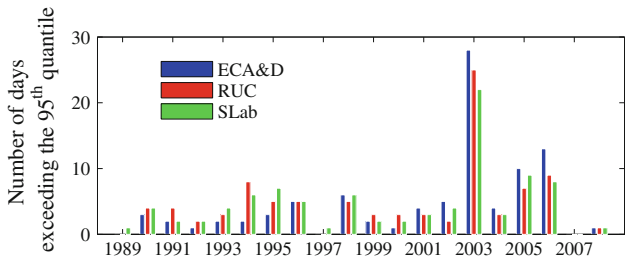

Fig. 4 Number of heatwave days (temperature anomaly exceeding the 95th quantile) for ECA&D data, RUC and SLab simulations

4 Sensitivity analysis

Investigating the differences between the RUC and SLab simulations allows a better understanding of the dynamical processes controlling the soil moisture/temperature feedbacks and their contribution to the temperature anomaly associated with the Heatwaves. The sensitivity analysis is performed on the days classified as Heatwave days in both RUC and SLab simulations. It includes 77 days among the main events that have been experienced in France in the 1989–2008 period (Stéfanon et al. 2012a). All the following figures in this section are displayed at 1200 UTC.

The atmospheric part of the model responds to a change of LSM via the change in the surface fluxes. Hence, we

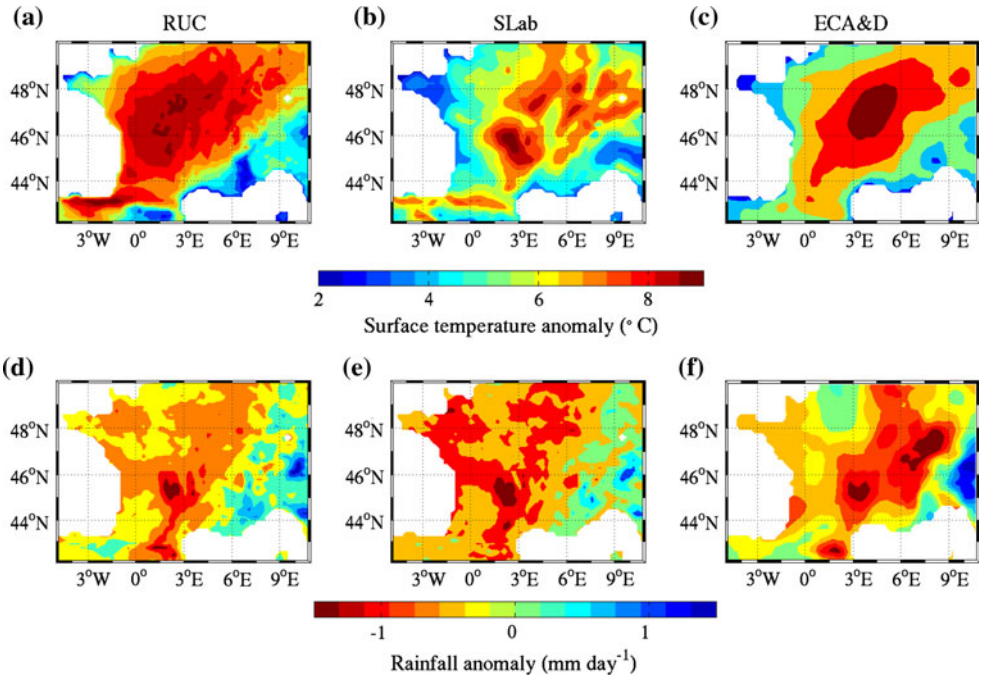

Fig. 5 2003 summer temperature (*upper row*; **a**, **b**, **c**) and precipitation (*lower row*; **d**, **e**, **f**) anomalies with respect to the heatwave climatology (1989–2008) from the RUC simulation (*left column*, **a**, **d**), the SLab simulation (*middle column*, **b**, **e**) and the ECA&D data (*right column*, **c**, **f**)

study here the sensitivity to a change of the Bowen ratio (the ratio of sensible to latent heat flux). RUC and SLab do not treat soil moisture in the same way. As mentioned, while RUC has a full model of soil hydrology, in SLab it is implicitly taken into account only as a coefficient in the bulk formulas for moisture fluxes. In this sense, the Bowen ratio is also a proxy for soil moisture availability, and a common measure to compare the two integrations in terms of sensitivity to soil moisture changes. In the following, we will employ the the concept of sensitivity to soil moisture and sensitivity to heat fluxes in a somewhat equivalent way.

Figure 6 displays the Bowen ratio *Bo* for the two simulations. In the SLab simulation, the Bowen ratio is very low (see Sect. 2). Except in very local spots (0.8 locally in the Alps, and 0.65 on average over the Alpine region), it hardly exceeds 0.5–0.6 meaning that evapotranspiration is limited by the downward solar energy (Seneviratne et al. 2010). In the RUC simulation, high Bowen ratio values (>5) are associated with very dry conditions in the flat plains of Southern France (South of 46°N latitude). North of 46°N latitude, the Bowen ratio still displays high values reaching on average 2. Bowen ratio values exceeding 2 refer to areas where evapotranspiration is limited by soil moisture deficit. Bowen ratio decreases with altitude down to 0.5, which marks a shift towards an evapotranspiration regime limited by the downward solar energy. In the Alps, the RUC Bowen ratio is lower than in SLab (0.65 and 0.97 respectively). Compared to the SLab simulation, the RUC simulation has a lower soil moisture availability in the lowlands with a much larger meso-scale spatial variability. This is directly caused by rainfall deficit preceding and during the Heatwaves generating significant soil moisture deficit (Vautard et al. 2007; Stéfanon et al. 2012a, b). The RUC simulation can thus be considered as a dry run whereas the SLab simulation can be considered as a wet run. However, in the mountains, the difference between the RUC and SLab simulations is smaller. The land use is dominated by forests having deep roots attenuating the effect of soil moisture deficit in the uppermost soil layers (Stéfanon et al. 2012b). Such differences affect the energy budget at the surface. Figure 7 details the patterns of the latent and sensible heat fluxes. It displays the difference of latent heat flux during the Heatwaves between the RUC and SLab simulations. The latent heat flux is much weaker in the RUC simulation, especially in South Western France and along the Mediterranean coast where the difference can reach -300 W m^{-2}. The differences between the two simulations weaken with altitude. Over the Massif Central, the difference decreases down to -100 W m^{-2}. It can even be higher in the RUC simulations at high altitude in the Alps and the Pyrénées with value reaching $+100$ W m^{-2}.

An indirect effect of such differences in the RUC and SLab simulations is the production of a larger amount of clouds over the Alps and the Pyrénées. Figure 7c shows the difference in downward solar radiation between RUC and SLab. The strongest differences are found over the Alps and the Pyrénées (-100 W m^{-2} on, average, and locally down to -250 W m^{-2}). Over moderate elevation mountains (Massif Central and Vosges), there is a slight negative difference of about -30 W m^{-2}. Elsewhere the differences are lower than 10 W m^{-2} in absolute value which is not

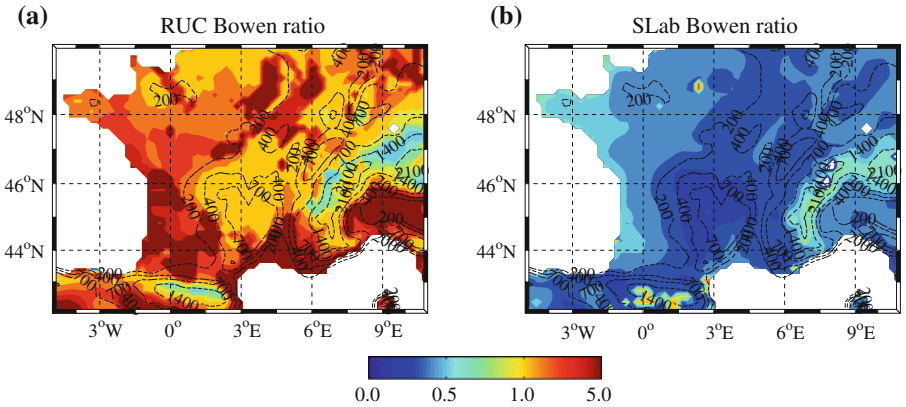

Fig. 6 Bowen ratio averaged over the Heatwave days during the 1989–2008 period from the RUC (**a**) and SLab (**b**) simulations. *Dashed lines* indicate the topography elevation

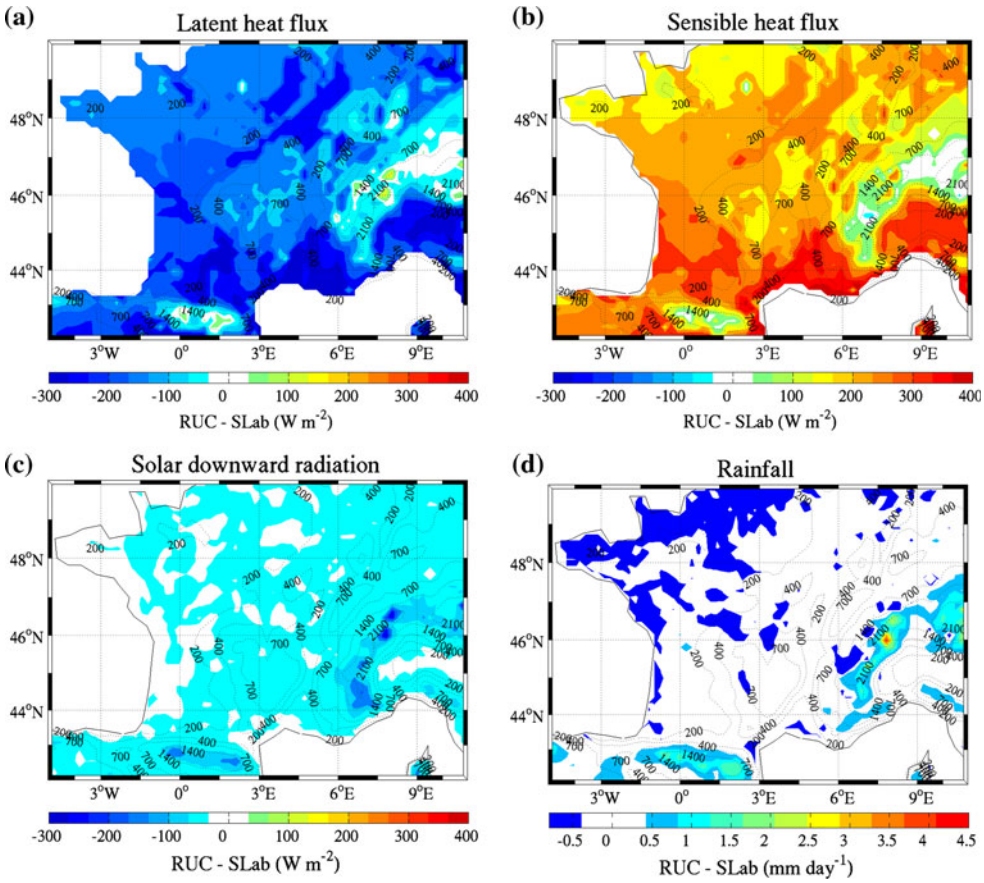

Fig. 7 Difference of surface latent (**a**) and sensible (**b**), downward solar radiation (**c**) and accumulated rainfall averaged over the Heatwave days of the 1989–2008 period between the RUC and SLab simulations. *Dashed lines* indicate the topography elevation

statistically significant. Figure 7d shows the difference in accumulated rainfall between RUC and SLab during the Heatwaves. The pattern is very similar to that of the latent heat flux or downward solar radiation differences. The RUC simulation produces more rainfall (about 70 mm over the 77 Heatwave days) than the SLab simulation over the most elevated peaks of the Pyrénées and the Alps. The difference can be as high as 300 mm over the 77 Heatwave days. The difference tends to zero over the lowlands and is slightly negative near the Atlantic and Mediterranean coasts. The analysis of the diurnal cycle of rainfall averaged over the domain (not shown) shows that during Heatwaves, hourly rainfall rate is 1.18 times larger in the RUC simulation than in SLab. The precipitation is mostly convective, the large scale precipitation representing less than 10 % of the total amount in both simulations. In the RUC simulation, the precipitation peak occurs between 1500 and 1800 UTC whereas in the SLab simulation precipitations are shorter and their maximum is reached around 1800 UTC. With respect to climatological summer rainfall, the precipitation amount during Heatwaves is 2.5 lower in the two simulations. It has been shown that

regarding precipitation, model results mostly depend on the parameterization of convection. However, it has been shown that KF scheme gives results similar to those produced by cloud resolving model (Bechtold et al. 2001; Guichard et al. 2004; Hohenegger et al. 2009).

Soil moisture thus strongly controls latent heat fluxes, as well as cloud formation and precipitation initiation. This feedback loop affects the transfer of sensible heat to the atmosphere and so the near surface temperature. In order to quantify the contribution of soil moisture availability on the Heatwave temperature anomaly we compute the index I_{SMTF} (SMTF standing for soil moisture-temperature feedback) defined as:

$$I_{SMTF}(\%) = 100 \times \frac{\Delta T_{RUC} - \Delta T_{SLab}}{\Delta T_{SLab}}$$

where ΔT_{RUC} and ΔT_{SLab} are the Heatwave temperature anomalies from the RUC and SLab simulations, respectively. Physically, ΔT_{SLab} is mainly driven by the synoptic conditions, the effect of soil moisture deficit being absent, whereas ΔT_{RUC} includes the impact of synoptic conditions and soil moisture effects. I_{SMTF} can be seen as the fraction of the additional Heatwave temperature anomaly that can be attributed to soil moisture-temperature feedbacks. Positive (resp. negative) values of I_{SMTF} mean that less soil moisture amplify (resp. damp) the amplitude of the Heatwaves. Figure 8 displays the spatial pattern of I_{SMTF}. In Western France, I_{SMTF} reaches values around 70 % which corresponds to a temperature anomaly warmer by about 3.5° C in the RUC simulation with respect to the SLab simulation. I_{SMTF} decreases eastwards. Averaging North of the mountains, I_{SMTF} is about 30–40 % which is consistent with the results of Fischer et al. (2007a, b). However, in mountains and Mediterranean regions I_{SMTF} takes negative values and can even be as low as −20 %. Such spatial pattern is robust and has been found for all simulated Heatwaves. There are thus evidences of significant meso-scale differences of the soil moisture-temperature feedbacks. The following section aims at understanding the underlying physical processes producing this variety of temperature response.

5 Analysis of meso-scale dynamical processes

Locally, surface air temperature is intimately linked to the surface energy budget and the partition between latent and sensible heat fluxes. This partition depends on the soil-moisture precipitation feedback, which is mainly controlled by local convective processes as discussed in the previous section. Regionally, the complex nature of the terrain (inland surface heterogeneities, land/sea contrast, elevated orography) induces meso-scale circulations as slope wind,

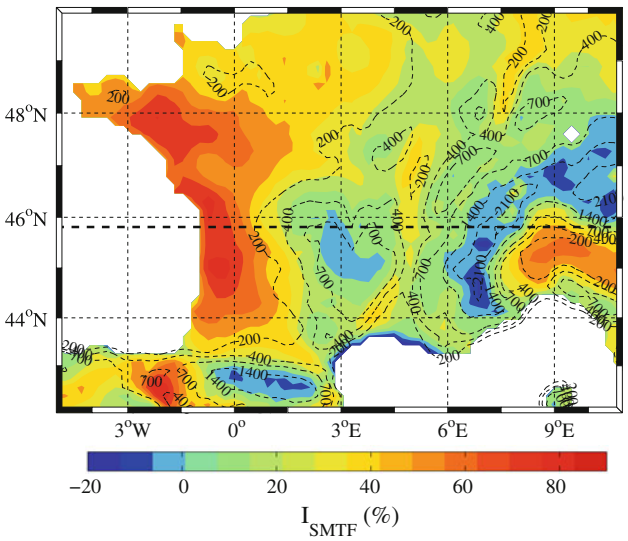

Fig. 8 Index I_{SMTF} averaged over the Heatwave days of the 1989–2008 period. The *thick dashed line* indicates the cross section at 45.8° N analyzed in Sect. 5. *Thin dashed lines* indicate the topography elevation

sea breeze and valley wind which can enhance locally vertical motion by wind convergence and also humidity transport from moist areas (e.g. Mediterranean Sea, Atlantic Ocean) to dry convective zones.

Figure 9 displays the planetary boundary layer (PBL) depth at 1500 UTC averaged over the Heatwaves days for the two simulations. It is computed in the boundary layer scheme as the height where a critical Richardson number is reached (Noh et al. 2003). The PBL depth over the sea is similar in the two simulations and is not shown. In SLab, the boundary layer depth remains low almost everywhere and hardly reaches 1,000 m. It slightly increases over the mountains and very locally can reach 1,500 m. While at few locations in the Alps the boundary layer can be slightly deeper in the SLab simulation than in the RUC simulation, it is in general much deeper in RUC. It is on average 2,200 m in the lowlands where surface sensible heat fluxes are much larger than in the SLab simulation (see Fig. 7b above). Values ranging between 1,200 and 1,800 m are found in the coastal regions and over the Alps. The highest values are up to 2,800 m in South-Western France, the Rhône Valley and the Po valley, also consistent with larger sensible heat flux (i.e. +350 W m $^{-2}$).

As an indicator of convective activity, we compute the level of free convection (LFC) at 1500 UTC. Figure 9 presents the exceedance rate of the LFC at the PBL top. Except over the Alps where it is on average 35 %, the probability that the PBL is higher than the LFC is zero in the SLab simulation. In RUC, the highest rate (60 %) are found over the Alps and the Pyrénées. Moderate elevation have a lower rate of about 35 % as over the Massif Central

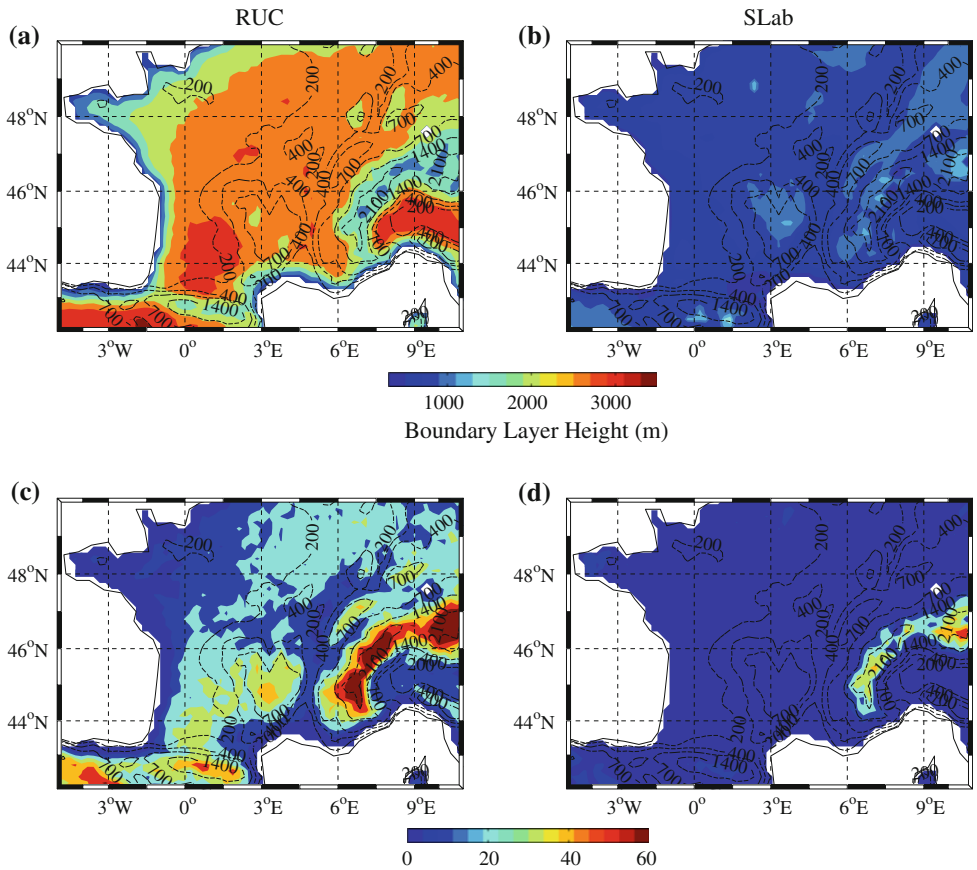

Fig. 9 Planetary boundary layer depth (**a**–**b**) and exceedance rate (%) of the level of free convection at the boundary layer top (**c**–**d**) at 1500 UTC, averaged over all Heatwaves days for the RUC (*right column* **a** and **c**) and SLab (*left column*; **b** and **d**) simulations. *Dashed lines* indicate the topography elevation

and over Jura and Vosges, in Eastern France. The rate is 10–20 % over the plains. The tendency to higher convective activity in RUC can also be diagnosed by computing convective available potential energy (CAPE) and convection inhibition (CIN) in the two simulations. This diagnostic (not shown) indicates higher values of CIN in SLab than in RUC. This explains the lower probability of convection triggering in SLab, despite the fact that higher values of CAPE are also observed there, which would indicate more—untriggered—potential for convection in SLab. In summary, both these analyses confirm a higher convective activity in the RUC simulation, in particular over the mountains but also on the rest of the domain, in agreement with Fig. 7.

Figure 10, panels a and b, shows the cross section at 45.8° N (Fig. 1b) of relative humidity (RH) with superimposed isentropes at 1500 UTC averaged over all heat wave days for the RUC and SLab simulations. The cross section goes through the plain and major mountains from west to east. In the RUC simulation a band of high RH appears at around 700–650 mb, corresponding to the top of the boundary layer. In correspondence with the orographic elevations, the local maxima of RH suggest higher probability of cloud formation. Conversely, in SLab relative humidity is confined within the boundary layer (Fig. 9b), reaching 50 % West of the Alps and 70 % South Alps. High relative humidity over drier soil has been observed before and interpreted as a tendency to higher shallow cloud cover (Ek and Holtslag 2004; Westra et al. 2012). The physical explanation of this behavior comes from an interplay of the effect of reduced evaporation, that tends to reduce relative humidity, and of entrainment of cold air from the boundary layer top that can increase it by lowering the saturation threshold. Under conditions of low instability, the second effect prevails, and the air column is in a regime of so-called "dry advantage" (Ek and Holtslag 2004; Gentine et al. 2012). Since RUC is considerably drier than SLab, shallow clouds are favored there.

Although the "dry advantage" condition is present everywhere in the domain, it is in particular in correspondence of the mountains that the RH is highest in Fig. 10, which suggests that an orographic contribution to cloud formation is also active. Panels c and d of Fig. 10

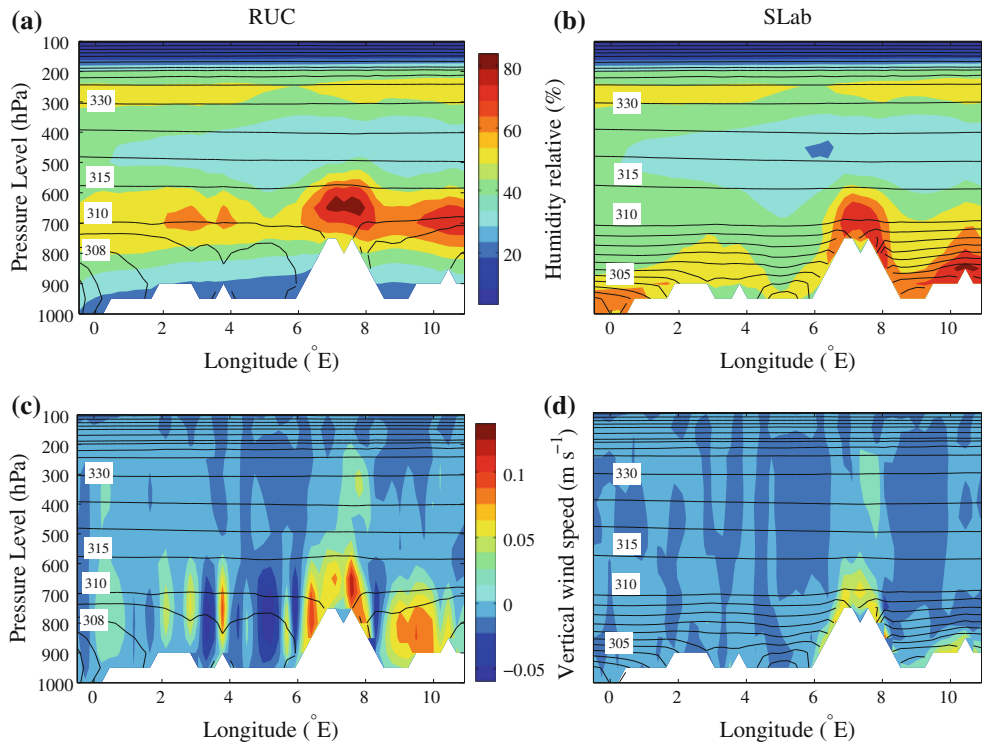

Fig. 10 Cross section at 45.8° N (Fig.1b) of relative humidity (**a**, **b**) and vertical velocity (**c**, **d**) in *color* with superimposed isentropes (isocontours of potential temperature) at 1500 UTC averaged over all Heatwave days for the RUC (*right column* **a**, **c**) and SLab (*left column*; **b**, **d**) simulations

display vertical velocity in the cross section for the two integrations. Convective motion is visible over mountains in RUC, with updrafts exceeding 6–8 cm s^{-1} with a maximum of 12 cm s^{-1} on the Eastern flank of the Alps. Conversely in SLab, no convection is triggered above terrain of moderate elevation. The isentropes show a cold and stratified atmospheric boundary layer, preventing any convective motion. Over the Alps, vertical motion is simulated but with speed lower than 5 cm s^{-1}. From the shape of the isentropes, this is not due to unstable boundary layer stratification but to upslope winds (i.e. anabatic winds). Such regional circulation between the Alps and the foreland is also referred as "Alpine pumping" and is known to increase convection and precipitation over the Alps (Raymond and Wilkening 1980; Weissmann et al. 2005; Bastin and Drobinski 2006). Combination of the anabatic wind mechanical forcing with the dry advantage regime described above, and the dry conditions of the RUC simulation, concur over the mountains to triggering shallow convection. This explains the increased cloud cover and precipitation over mountains in RUC, as well as the somewhat counter-intuitive result that under heat wave conditions and dry soil, temperature can sometimes be locally reduced.

For a more in-depth analysis, we show the diurnal cycle of the surface energy budget at specific locations in the Alps (A–B), the Massif central (C), in the plain (D) and near the Mediterranean coast at the exit of the Rhône valley (E) (see locations in Fig. 1b). Figure 11 shows the mean diurnal cycle of the difference of the solar downward radiation, latent and sensible heat fluxes between the RUC and SLab simulations. The difference of temperature anomaly is also superposed. In the mountains (locations A, B and C), Fig. 11 shows that the temperature anomaly is much larger in the RUC simulation at night than in the SLab simulation. This difference decreases significantly during the day and reaches a minimum at the warmest period of the day (between 1200 and 1500 UTC). This evolution is similar at all mountain locations. However the difference of temperature anomaly shifts towards negative values with increasing altitude. At location A at 2,500 m height, the difference of temperature anomaly between the RUC and SLab simulations can reach −1 °C at 1200 UTC. The minimum of temperature anomaly reaches +0.2 and +1 °C at 1200 UTC at locations B and C at 2,100 and 750 m height, respectively. At these locations, latent heat flux becomes larger in the RUC simulation than in the SLab simulation by 50 W m s^{-2} at about 1800 UTC, during the rainfall events. This is associated with an important decrease of solar downward radiation (−86 W m s^{-2} at location B) which starts at 1200 UTC since the clouds form earlier in the RUC simulations. Sites D and E are located at about 50 m height.

The evolution of the difference of temperature anomaly between the RUC and SLab simulations in coastal areas at locations D and E differs from that at the mountain sites. At location D, in the plain west of the Atlantic coast, the temperature anomaly difference is the highest and can reach +3.5 °C around 1200 UTC when the difference of downward solar radiation between the RUC and SLab simulations is also the highest. The downward solar radiation is more important during the early morning in the RUC simulation, owing to the presence of fog in the SLab simulation. This lack of cloudiness and the deficit in soil moisture contributes to the build up of daytime heat at 1200 UTC, with an increase of sensible heat flux at the expense of latent heat flux. Contrary to the situation in mountains, the difference of temperature anomaly is minimum at night and increases during the day as expected in the case of positive soil moisture/temperature feedback.

Near the Mediterranean coast (location E), the evolution of the different terms of the energy budget differs from all previous cases. The difference of temperature anomaly remains negative and decreases from 0900 UTC down to −1.2 °C at 1800 UTC. It corresponds to the hour of maximum sea breeze in this region (Bastin et al. 2005a, b; Bastin and Drobinski 2006; Drobinski et al. 2006). The sea breeze is induced by a temperature gradient between the air temperature above sea and land. In the RUC and SLab simulations, the SST is prescribed from ERA-Interim reanalysis. The larger temperature from the RUC simulation above land due to reduced evaporation and enhanced sensible heat flux with respect to the SLab simulation, strengthens this sea-breeze circulation in all the coastal areas. This is illustrated in Fig. 12 which shows the near-surface horizontal wind averaged over the Heatwave days from RUC and SLab simulations. Advection of moist and cool marine air by the sea-breeze cools down the atmospheric boundary layer over land over a horizontal range that can exceed 150 km inland as shown in Fig. 12 (Drobinski et al. 2006; Drobinski and Dubos 2009). This confirms the impact of the sea-breeze on the generation of slope winds over the mountains surrounding the Mediterranean coast, as discussed earlier. Locations D and E are thus both under the influence of the sea-breeze circulation, however the differences of temperature anomaly have no similar evolution (Fig. 11).

In these areas, the effects of two opposing processes—soil heating and breeze cooling—are active against each other. For the Atlantic area in RUC, a positive sensible heat flux anomaly increases the temperature anomaly and the sea-breeze tends to reduce it. This is not the case for the Mediterranean area; here, the soil moisture is low during all summers, be it heatwaves or not. Hence, there is no sensible heat flux anomaly and the damping effect by cool air advection is more effective in decreasing the temperature anomaly. For the Mediterranean area in SLab, there is also no sensible heat flux anomaly since in this case the soil moisture is always high. However, the damping effect is lower than in RUC since the land sea thermal contrast is also lower. The effect of coastal cooling versus inland warming has been documented by Lebassi et al. (2009) for California, although not specifically during heat waves.

6 Summary and conclusions

This paper investigates the impact of soil moisture-temperature feedback at meso-scale on the Heatwaves occurring over Western Europe between 1989 and 2008. We use two simulations performed in the framework of HyMeX and MED-CORDEX programs with the two different land-surface models. The first land-surface model resolves the hydrology and is able to simulate the summer dryness, whereas the second land-surface model prescribes a constant and high soil moisture availability which prevents the simulation of soil moisture deficit. A sensitivity analysis

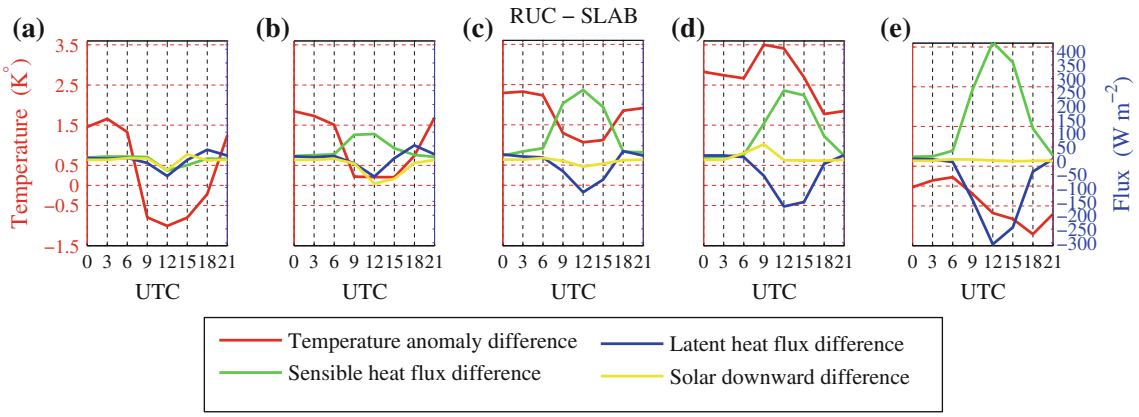

Fig. 11 Diurnal cycle of the difference of temperature anomaly (*red*), sensible (*green*) and latent (*blue*) heat fluxes and shortwave radiation (*yellow*) between the RUC and SLab simulations averaged over all Heatwave days, at locations **a**, **b**, **c**, **d** and **e** indicated in Fig. 1b

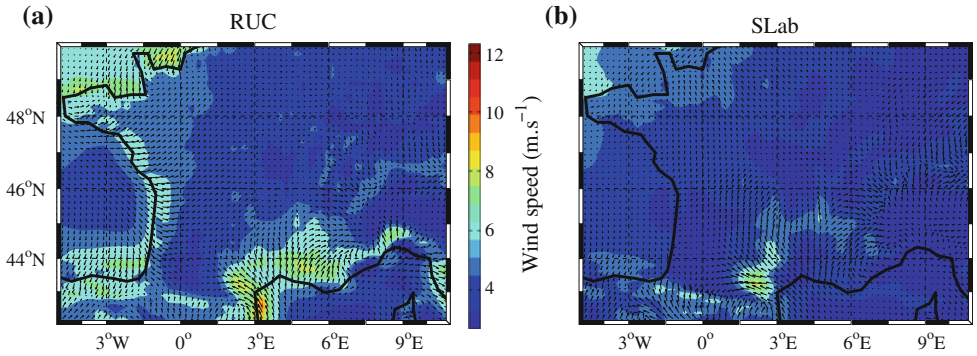

Fig. 12 Near-surface horizontal wind vectors averaged over all Heatwave days at 1800 UTC from the RUC (**a**) and SLab (**b**) simulations. The *color shading* indicates the wind speed in in m s $^{-1}$

highlights different soil moisture-temperature responses (1) over low-elevation plains, (2) over mountains and (3) over coastal regions.

In the lowlands, the dominant process is the conversion of solar radiation into heat at the expense of evapotranspiration, which is very low due to the soil-moisture deficit. Soil moisture deficit induces less evapotranspiration, a drier atmosphere and therefore less clouds and precipitation. A positive feedback loop is thus created. This well-known process is found to contribute to 20 % of the temperature anomaly in Eastern France and Western Germany, and to 40 % of the temperature anomaly in Western France and Northern Spain during the Heatwave; the initial cause of the Heatwave remaining the presence of a persisting synoptic blocking situation over the region of the Heatwave. A less intuitive result is the presence of high relative humidity at the top of the boundary layer over drier soil. The physical explanation of this behavior comes from an interplay of the effect of reduced evaporation, that tends to reduce relative humidity, and of entrainment of cold air from the boundary layer top that can increase it by lowering the saturation threshold. Under conditions of low instability, the second effect prevails, and the air column is in a regime of so-called "dry advantage".

Over the mountains surrounding the Mediterranean coast (Pyrénées, Massif Central and the Alps), the relative humidity is highest, which suggests that an orographic contribution to cloud formation is also active. Enhanced heat fluxes over dry soil reinforce anabatic winds. Combination of the anabatic wind mechanical forcing with the dry advantage regime concur over the mountains to triggering shallow convection. This negative feedback loop explains the increased cloud cover and precipitation over mountains under Heatwave conditions and dry soil, and locally the lower temperature.

Finally, in coastal regions, the land/sea thermal contrast is enhanced in case of dry soil, strengthening sea-breeze circulation and moist cold marine air advection. This damps the magnitude of the Heatwave temperature anomaly over a narrow land band near the Atlantic coast and even decreases by 25 % the temperature anomaly near the Mediterranean coast.

This study thus highlights the significant impact of meso-scale dynamics on the soil moisture-temperature feedback. These meso-scale circulations like slope winds and sea-breeze can modulate the well-known local soil-atmosphere feedback by the generation of wind convergence and the advection of moist air from remote regions (e.g. oceans). Wind convergence induced by meso-scale circulations contributes to enhance vertical motion and facilitate convection initiation and precipitation which in turn cool down the atmosphere. Moisture advection can increase moist static energy over convective dry areas also favoring shallow convection and precipitation.

In this study, we take advantage of 20-years simulations performed at 20 km resolution to extract the most significant meso-scale dynamical processes associated with Heatwaves and not focus on case sensitive processes associated with one particular event. The main drawback of this approach is that despite the fairly "high" resolution, the simulations still rely on convection parameterization. We took care to use convection parameterization that has been shown to produce results which are consistent with results from cloud resolving models. Nevertheless, uncertainties remain associated with the representation of the hydrological cycle and the land atmosphere coupling in regional climate models. Especially, soil moisture conditions depend considerably on the level of sophistication of the land-surface model.

Most land-surface models simulate the exchange of surface water and energy fluxes at the soil-atmosphere interface and do not account for water redistribution by rivers, vegetation phenology and dynamics. Accounting for these processes can modify by few tens of percent the temperature anomaly of a Heatwave, impact water exchange between the soil and the atmosphere and

modulate the life cycle of droughts and Heatwaves (Stéfanon et al. 2012b). Only long-term simulations at the meso-scale taking this elaborate effects into account can contribute in the future to discriminate the robust processes involved in the land-atmosphere interaction from weaker ones.

Acknowledgments This work is a contribution to the MORCE-MED and Humboldt projects funded by the GIS (Groupement d'Intérêt Scientifique) "Climat, Environnement et Société", with granted access to the HPC resources of IDRIS (under allocation i2011010227). This work also contributes to the HyMeX program (HYdrological cycle in The Mediterranean EXperiment - Drobinski et al (2010); Drobinski et al (2012)-http://www.hymex.org) through INSU-MISTRALS support, the Med-CORDEX program (A COordinated Regional climate Downscaling EXperiment - Mediterranean region, http://www.medcordex.eu) and the GEWEX program of the World Climate Research Program (WCRP).

References

Bastin S, Drobinski P (2005) Temperature and wind velocity oscillations along a gentle slope during sea-breeze events. Bound-Layer Meteorol 114:573–594

Bastin S, Drobinski P (2006) Sea-breeze-induced mass transport over complex terrain in south-eastern france: a case-study. Q J R Meteorol Soc 132:405–423

Bastin S, Champollion C, Bock O, Drobinski P, Masson F (2005a) On the use of gps tomography to investigate water vapor variability during a mistral/sea breeze event in southeastern france. Geophys Res Lett 32:L05808. doi:10.1029/2004GL021907

Bastin S, Drobinski P, Dabas A, Delville P, Reitebuch O, Werner C (2005b) Impact of the rhône and durance valleys on sea-breeze circulation in the marseille area. Atmos Res 74:303–328

Bastin S, Champollion C, Bock O, Drobinski P, Masson F (2007) Diurnal cycle of water vapor as documented by a dense gps network in a coastal area during escompte-iop2. J Appl Meteorol Climatol 46:167–182

Bechtold P, Bazile E, Guichard F, Mascart P, Richard E (2001) A mass-flux convection scheme for regional and global models. Q J R Meteorol Soc 127:869–886

Beljaars A, Viterbo P, Miller M, Betts A (1996) The anomalous rainfall over the united states during july 1993: sensitivity to land surface parameterization and soil moisture anomalies. Mon Wea Rev 124:362–383

Beniston M (2004) The 2003 heat wave in europe: a shape of things to come? An analysis based on swiss climatological data and model simulations. Geophys Res Lett 31:L02202. doi:10.1029/2003GL018857

Betts AK, Ball JH, Beljaars ACM, Miller MJ, Viterbo PA (1996) The land surface-atmosphere interaction: a review based on observational and global modeling perspectives. J Geophys Res 101:7209–7225

Bleck R, Benjamin SG (1993) Regional weather prediction with a model combining terrain-following and isentropic coordinates. i: model description. Mon Wea Rev 121:1770–1785

Bradley CM (2003) Effects of soil data resolution on modeling results using a physically based rainfall-runoff model. Master's thesis, University of Arizona, Tucson

Cassou C, Terray L, Phillips AS (2005) Tropical atlantic influence on european heatwaves. J Climate 18:2805–2811

Chagnon FJF, Bras RL, Wang J (2004) Climatic shift in patterns of shallow clouds over the amazon. Geophys Res Lett 31:1183–1199

Christensen JH, Christensen OB (2003) Severe summertime flooding in europe. Nat Biotechnol 421:805–806

Couvreux F, Guichard F, Autsin P, Chen F (2009) Nature of the meso-scale boundary layer height and water-vapor variability observed the 14 June 2002 during the ihop 2002 campaign. Mon Wea Rev 137:414–432

Couvreux F, Rio C, Guichard F, Lothon M, Canut J, Bouniol D, Gounou A (2012) Initiation of daytime local convection in a semi-arid region analysed with high-resolution simulation and amma observations. Q J R Meteorol Soc 138:56–71

D'Andrea F, Provenzale A, Vautard R, De Noblet-Decoudré N (2006) Hot and cool summers: multiple equlibria of the continental water cycle. Geophys Res Lett 33:L24,807

Dee DP, Uppala SM, Simmons AJ, Berrisford P, Poli P, Kobayashi S, Andrae U, Balmaseda MA, Balsamo G, Bauer P, Bechtold P, Beljaars ACM, van de Berg L, Bidlot J, Bormann N, Delsol C, Dragani R, Fuentes M, Geer AJ, Haimberger L, Healy SB, Hersbach H, Hólm EV, Isaksen L, Kållberg P, Köhler M, Matricardi M, McNally AP, Monge-Sanz BM, Morcrette JJ, Park BK, Peubey C, de Rosnay P, Tavolato C, Thépaut JN, Vitart F (2011) The era-interim reanalysis: configuration and performance of the data assimilation system. Q J R Meteorol Soc 137:553–597

Della-Marta PM, Haylock MR, Luterbacher J, Wanner H (2007) Doubled length of western european summer heat waves since 1880. J Geophys Res 112:D15103. doi:10.1029/2007JD008510

Drobinski P, Dubos T (2009) Linear breeze scaling: From large-scale land/sea-breezes to mesoscale inland breezes. Q J R Meteorol Soc 135:1766–1775

Drobinski P, Flamant C, Dusek J, Flamant P, Pelon J (2001) Observational evidence and modeling of an internal hydraulic jump at the atmospheric boundary layer top during a tramontane event. Boundary Layer Meteorol 98:497–515

Drobinski P, Bastin S, Guénard V, Caccia J, Dabas AM, Delville P, Protat A, Reitebuch O, Werner C (2005) Summer mistral at the exit of the rhône valley. Q J R Meteorol Soc 131:353–375

Drobinski P, Bastin S, Dabas A, Delville P, Reitebuch O (2006) Variability of three-dimensional sea breeze structure in southern france: observations and evaluation of empirical scaling laws. Ann Geophys 24:1783–1799

Drobinski P, Ducrocq V, Lionello P, the HyMeX ISSC (2009) Hymex, a potential new CEOP RHP in the mediterranean basin. GEWEX Newslett 19:5–6

Drobinski P, Ducrocq V, Lionello P (2010) Studying the hydrological cycle in the mediterranean. Trans Am Geophys Union (EOS) 91:373

Drobinski P, Anav A, Lebeaupin Brossier C, Samson G, Stéfanon M, Bastin S, Baklouti M, Béranger K, Beuvier J, Bourdallé-Badie R, Coquart L, D'Andrea F, De Noblet-Ducoudré N, Diaz F, Dutay JC, Ethe C, Foujols AM, Khvorostyanov D, Madec G, Mancip M, Masson S, Menut L, Palmieri J, Polcher J, Turquety S, Valcke S, Viovy N (2012) Model of the regional coupled earth system (morce): application to process and climate studies in vulnerable regions. Environ Model Soft 35:1–18

Dudhia J (1989) Numerical study of convection observed during the winter monsoon experiment using a mesoscale two-dimensional model. J Atmos Sci 46:3077–3107

Easterling DR, Meehl GA, Parmesan C, Changnon SA, Karl TR, O ML (2000) Climate extremes: observations, modeling, and impacts. Sci Agric 289:2068–2074

Eckel T (2002) Perturbing mm5 moisture availability for ensemble forecasting. Technical Report, University of Washington

Ek MB, Holtslag AAM (2004) Influence of soil moisture on boundary layer cloud development. J Hydrometeor 5:86–89

Findell KL, Eltahir EAB (2003) Atmospheric controls on soil moisture boundary layer interactions. part i: framework development. J Hydrometeorol 4:552–569

Fink AH, Bruecher T, Leckebusch GC, Krueger A, Pinto JG, Ulbrich U (2004) The 2003 european summer heatwaves and drought-synopstic diagnosis and impacts. Weather 59:209–216

Fischer EM, Seneviratne SI, Lüthi D, Schär C (2007a) Contribution of land-atmosphere coupling to recent European summer heat waves. Geophys Res Lett 34:L06707. doi:10.1029/2006GL029068

Fischer EM, Seneviratne SI, Vidale PL, Lüthi D, Schär C (2007b) Soil moisture–atmosphere interactions during the 2003 european summer heat wave. J Clim 20:5081–5099

Fouillet A, Rey G, Laurent F, Pavillon G, Bellec S, Guihenneuc-Jouyaux C, Clavel J, Jougla E, Hémon D (2006) Excess mortality related to the august 2003 heat wave in France. Int Arch Occup Environ Health 80:16–24

Gentine P, Holtslag A, D'Andrea F, Ek M (2012) Surface and atmospheric controls on moist convection onset over land. J Hydrometeor (submitted)

Giorgi F, Jones C, Asrar GR (2009) Addressing climate information needs at the regional level: the cordex framework. WMO Bull 58:175–183

Guénard V, Drobinski P, Caccia J, Campistron B, Bénech B (2005) An observational study of the mesoscale mistral dynamics. Boundary Layer Meteorol 115:263–288

Guénard V, Drobinski P, Caccia J, Tedeschi G, Currier P (2006) Dynamics of the map iop-15 severe mistral event: observations and high-resolution numerical simulations. Q J R Meteorol Soc 132:757–778

Guichard F, Petch JC, Redelsperger JL, Bechtold P, Chaboureau JP, Cheinet S, Grabowski W, Grenier H, Jones CG, Köhler M, Piriou JM, Tailleux R, Tomasini M (2004) Modelling the diurnal cycle of deep precipitating convection over land with cloud-resolving models and single-column models. Q J R Meteorol Soc 130:3139–3172

Guichard F, Kergoat L, Mougin E, Timouk F, Baup F, Hiernaux P, Lavenu F (2009) Surface thermodynamics and radiative budget in the sahelian gourma: seasonal and diurnal cycles. J Hydrology 375:161–177

Haylock MR, Hofstra N, Klein Tank AMG, Klok EJ, Jones PD, New M (2008) A European daily high-resolution gridded data set of surface temperature and precipitation for 1950–2006. J Geophys Res 113:D20119

Hohenegger C, Brockhaus P, Bretherton CS, Schär C (2009) The soil moisture–precipitation feedback in simulations with explicit and parameterized convection. J Climate 22:5003–5020

Hong SY, Pan HL (1996) Nonlocal boundary layer vertical diffusion in a medium-range forecast model. Monthly Wea Rev 124(10):2322–2339

Hong SY, Dudhia J, Chen SH (2004) A revised approach to ice microphysical processes for the bulk parameterization of clouds and precipitation. Mon Wea Rev 132:103–120

Hong SY, Noh Y, Dudhia J (2006) A new vertical diffusion package with an explicit treatment of entrainment processes. Mon Wea Rev 134(9):2318–2341

Kain JS (1993) Convective parameterization for mesoscale models : The kain-fritsch scheme. The representation of cumulus convection in numerical models http://ci.nii.ac.jp/naid/10014597699/en/

Kain JS (2004) The kain-fritsch convective parameterization: an update. J Appl Meteorol 43:170–181

Köppen W (1936) Das geographisca system der klimate. Handbuch der Klimatologie 25:1–44

Lebassi B, Gonzalez J, Fabris D, Maurer E, Miller N, Milesi C, Switzer P, Bornstein R (2009) Observed 1970–2005 cooling of summer daytime temperatures in coastal california. J Clim 22(13):3558–3573

Mahrt L, Pan HL (1984) A two-layer model of soil hydrology. Bound-Layer Meteor 29:1–20

Mlawer EJ, Taubnam SJ, Brown PD, J IM, A CS (1997) A validated correlated k-model for the longwave. J Geophys Res 102:1663–1682

Monin AS, Obukhov AM (1954) Basic laws of turbulent mixing in the surface layer of the atmosphere. Contrib Geophys Inst Acad Sci 151:163–187

Noh Y, Cheon WG, Hong SY, Raasch S (2003) Improvement of the k-profile model for the planetary boundary layer based on large eddy simulation data. Bound-Lay Meteorol 107:401–427

Omrani H, Drobinski P, Dubos T (2012) Investigation of indiscriminate nudging and predictability in a nested quasi-geostrophic model. Q J R Meteor Soc 138:158–169

Pal J, Eltahir E (2001) Pathways relating soil moisture conditions to summer rainfall within a model of the land-atmosphere system. J Clim 14:1227–1242

Peel MC, Finlayson BL, McMahon TA (2007) Updated world map of the Köppen-geiger climate classification. Hydrol Earth Syst Sci Discuss 4:439–473

Philip JR, de Vries DA (1957) Moisture movement in porous materials under temperature gradients. Trans Am Geophys Union (EOS) 38:222–232

Rabin RM, Stensrud DJ, Stadler S, Wetzel PJ, Gregory M (1990) Observed effects of landscape variability on convective clouds. Bull Am Meteorol Soc 71:272–280

Raymond D, Wilkening M (1980) Mountain-induced convection under fair weather conditions. J Atmos Sci 37:2693–2706

Salameh T, Drobinski P, Dubos T (2010) The effect of indiscriminate nudging time on large and small scales in regional climate modelling: Application to the mediterranean basin. Q J R Meteorol Soc 136:170–182

Santanello Jr JA, Peters-Lidard CD, Kumar SV (2011) Diagnosing the sensitivity of local land-atmosphere coupling via the soil moisture-boundary layer interaction. J Hydrometeorol 12(5):766–786

Schär C, Lüthi D, Beyerle U, Heise E (1999) The soil–precipitation feedback: a process study with a regional climate model. J Climate 12:722–741

Seneviratne SI, Lüthi D, Litschi M, Schär C (2006) Land-atmosphere coupling and climate change in europe. Nat Biotechnol 443:205–209

Seneviratne SI, Corti T, Davin EL, Hirschi M, Jaeger EB, Lehner I, Orlowsky B, Teuling AJ (2010) Investigating soil moisture-climate interactions in a changing climate: a review. Earth Sci Rev 99:125–161

Simons A, Uppala S, Dee D, Kobayashi S (2007) Era-interim: new ecmwf reanalysis products from 1989 onwards. ECMWF Newslett 110:25–35

Siqueira M, Katul G, Porporato A (2009) Soil moisture feedbacks on convection triggers: the role of soil-plant hydrodynamics. J Hydrometeorol 10(1):96–112

Skamarock WC, Klemp JB, Dudhia J, Gill DO, Barker DM, Duda MG, Huang XY, Wang W, Powers JG (2008) A description of the advanced research wrf version 3. Technical Report, NCAR

Smirnova TG, Brown JM, Benjamin SG (1997) Performance of different soil model configurations in simulating ground surface temperature and surface fluxes. Mon Wea Rev 125:1870–1884

Smirnova TG, Brown JM, Benjamin SG, Kim D (2000b) Parameterization of cold season processes in the maps land-surface scheme. J Geophys Res 105:4077–4086

Stauffer D, Seaman N (1990) Use of four-dimensional data assimilation in a limited-area mesoscale model. part i: experiments with synoptic-mesoscale data. Mon Wea Rev 118:1250–1277

Stéfanon M, D'Andrea F, Drobinski P (2012a) Heatwave classification over europe and the mediterranean region. Environ Res Lett 7(1):014023. doi:10.1088/1748-9326/7/1/014023

Stéfanon M, Drobinski P, D'Andrea F, Noblet-Ducoudré N (2012b) Effects of interactive vegetation phenology on the 2003 summer heat waves. J Geophys Res Atmos (1984–2012) 117(D24)

Tank AMGK, Wijngaard JB, Können GP, Böhm R, Demarée G, Gocheva A, Mileta M, Pashiardis S, Hejkrlik L, Kern-Hansen C, Heino R, Bessemoulin P, Müller-Westermeier G, Tzanakou M, Szalai S, Pálsdóttir T, Fitzgerald D, Rubin S, Capaldo M, Maugeri M, Leitass A, Bukantis A, Aberfeld R, van Engelen AFV, Forland E, Mietus M, Coelho F, Mares C, Razuvaev V, Nieplova E, Cegnar T, López JA, Dahlström B, Moberg A, Kirchhofer W, Ceylan A, Pachaliuk O, Alexander LV, Petrovic P (2002) Daily dataset of 20th-century surface air temperature and precipitation series for the European climate assessment. Int J Climatol 22:1441–1453

Taylor CM, Parker DJ, Harris PP (2007) An observational case study of mesoscale atmospheric circulations induced by soil moisture. Geophys Res Lett 34:L15,801

Troen I, Mahrt L (1986) A simple model of the atmospheric boundary layer; sensitivity to surface evaporation. Boundary-Layer Meteorol 37(1):129–148

Vautard R, Yiou P, D'Andrea F, de Noblet N, Viovy N, Cassou C, Polcher J, Ciais P, Kageyama M, Fan Y (2007) Summertime european heat and drought waves induced by wintertime mediterranean rainfall deficit. Geophys Res Lett 34:L07711. doi:10.1029/2006GL028001

Wang J, Chagnon FJF, Williams ER, Betts AK, Renno NO, Machado LAT, Bisht G, Konx R, Bras RL (2009) Impact of deforestation in the amazon basin on cloud climatology. Proc Natl Acad Sci 106:3670–3674

Weissmann M, Braun FJ, Gantner L, Mayr GJ, Rahm S, Reitebuch O (2005) The alpine mountain-plain circulation: airborne Doppler Lidar measurements and numerical simulations. Mon Wea Rev 133:3095–3109

Westra D, Steeneveld GJ, Holtslag AAM (2012) Some observational evidence for dry soils supporting enhanced high relative humidity at the convective boundary layer top. J Hydrometeor 13:1347–1358

Zampieri M, D'Andrea F, Vautard R, Ciais P, de Noblet-Ducoudré N, Yiou P (2009) Hot european summers and the role of soil moisture in the propagation of mediterranean drought. J Climate 22:4747–4758